

Small Closed-Form CI Expansions for Electronic g-Tensor Calculations

Gerald H. Lushington*

Ohio Supercomputer Center, 1224 Kinnear Road, Columbus, Ohio 43212-1163

Received: October 22, 1999; In Final Form: December 22, 1999

In recent years, major progress has been made toward devising accurate and practical computational methods for predicting electronic g-tensors of molecules, thus raising hopes of extending the capability to solid-state defects and solvated radicals. The best agreement with experiment has been obtained at the multireference configuration interaction level via explicit sum-over-states (SOS) expansions. This method is computationally very intensive, however, and the explicit expansion may prove unworkably convoluted for larger, more complex species. SOS perturbation expansions of g-tensors are dominated by states that magnetically couple with the ground state. For this reason, one may optimize g-tensor expansions by neglecting configurations not coupled magnetically with the ground state. This criterion yields a configuration space that is specially tailored to magnetic response, yet is small enough to allow for a closed-form configuration interaction (CFCI) treatment of the entire resulting excited-state manifold. This CFCI method has been applied herein to predict g-tensors for H_2O^+ , MgF, NO_2 , CO^+ , and H_2CO^+ . CFCI results compare very favorably with other high-level theoretical methods and are clearly superior to Restricted Open Shell Hartree Fock (ROHF) treatment, for which new numbers are reported herein. Expansions limited to one-open-shell determinants yield excellent results for H_2O^+ and MgF and decent values for CO^+ and NO_2 . Additional three-open-shell configurations improve results for both CO^+ and NO_2 , and do not significantly undermine the good agreement in H_2O^+ and MgF. H_2CO^+ , however, remains problematic within this formalism, probably due either to the shortcomings of the uncorrelated ground state or in the approximate treatment of the excited manifold.

Introduction

The electronic g-tensor is a parameter of electron paramagnetic resonance (EPR) spectroscopy that describes the location of absorption patterns or bands in the EPR spectrum. Perturbations imparted by the local atomic environment on the unpaired electrons in a paramagnetic center lead to deviations (g-shifts) in the positions of spectral features relative to those characteristic of free electrons. Contained within these g-shifts is useful information regarding the electronic and magnetic structure of the paramagnetic center.¹ Such information can be important for supplementing other spectroscopic techniques in the study of gaseous, solvated, and adsorbed radicals, and may prove vital in structural elucidation of complex bioradicals and solid-state paramagnetic defects.

Because g-shifts arise as the sum of various competing magnetic dipoles and relativistic effects, it can be difficult to pinpoint the exact relation between the g-tensor and underlying physical structure of the system. Accompanying theoretical g-tensor investigations can be very useful in deconvoluting such relations, however, by providing a detailed breakdown of different magnetic contributions.² For this reason, and because of the importance of the g-tensor to structural analysis, a capacity for reliable g-tensor computations in systems ranging from small isolated radicals to sizable complex clusters may prove valuable to numerous technologically important endeavors.

To date, the most accurate theoretically determined g-tensor results appear to be those obtained by treating the molecular magnetic response via a sum-over-states (SOS) perturbation expansion of explicitly resolved multireference configuration

interaction (MRCI) wave functions.^{3,4} For small molecules, the MRCI methodology has reproduced large experimental g-shifts to within about 20%, and small g-shifts to within several hundred parts per million (ppm) with fair consistency^{3–6}—error ranges that are close to the realm of experimental uncertainty.

One problem with the MRCI scheme is computational expense, which scales rather unfavorably with system size as approximately $O[N_{\text{R}}n^2N^4(n - N/2)^2]$ where N_{R} is the number of reference configurations, N is the number of electrons, and n is the number of orbitals.⁷ A further limitation lies with the issue of selecting the manifold of states to be included in the SOS expansion. Although the contributions of states are somewhat inversely dependent on excitation energy, lowest energy states are not always the largest contributors, and states at high (even nonphysical) energy levels sometimes contribute significantly because of strong spin-orbit and magnetic dipole coupling with the ground state.³ Unless one can reliably treat the entire state manifold (currently either impractical or impossible for all but the smallest molecules), one must impose a truncation scheme (e.g., as described in ref 3) wherein higher energy (generally weaker coupling) states are discarded. This leads to neglect of a portion of the contributions made by magnetically relevant configurations. As larger, more complex systems will likely require more drastic truncation, greater neglect will occur; thus it is unclear whether the MRCI scheme will prove extensible much beyond the small polyatomic molecules studied thus far.^{3–6}

Other recent high-level g-tensor calculations include ROHF SOS,^{8–10} coupled perturbed Hartree–Fock (CPHF),^{9,11} density-functional,^{12,13} and multiconfigurational linear response¹⁴ studies. Among these, the first three are the most computationally expedient, with scaling behavior in the range of $O[n^3]$ to $O[n^4]$.

* Fax: 614-292-7168; e-mail: gerald@osc.edu.

In terms of accuracy, the ROHF method appears to be generally capable of reproducing broad trends in g-shifts, but actual results often differ quantitatively with experiment by upward of 50% on large g-shifts.¹¹ The density functional theory (DFT) and CPHF methodologies provide a significant improvement over ROHF, but in general the quantitative agreement with experiment is not on par with that of the MRCI.^{3–6,9–13} The multiconfigurational linear response technique should exhibit accuracy comparable with that of MRCI, but may also become computationally very demanding, as the expense of the underlying multiconfigurational treatment can range up to an exponential dependency on the number of electrons in the system¹⁵ for some implementations.

In exploring alternatives to the above array of methods, a new technique has been developed and is described in this paper. It has a computational efficiency little different from the various single determinant approaches such as ROHF, CPHF, and DFT, but appears somewhat more accurate. The method essentially entails a configuration interaction SOS expansion wherein magnetic response is reproduced by coupling between the ground-state and excited-state manifold. It differs from the MRCI methodology, however, by expanding the excited manifold over a much smaller configuration space that has been specifically tailored to the magnetic response nature of the problem at hand. This tailoring is accomplished by restricting the configuration space to include only those determinants that couple magnetically to the single determinant (ROHF) unperturbed ground-state wave function. The small configuration space resulting from this restriction leads to a computationally manageable formalism that, by virtue of its specialized nature, still describes the magnetic response behavior with reasonable fidelity.

Theoretical Treatment

As is well-known, the Zeeman effect of EPR spectroscopy results from resonance between spin projections of a spin multiplet, energetically split as follows:

$$\Delta E = \mu_B \vec{S} \times \mathbf{g} \times \vec{B} \quad (1)$$

by the presence of an external magnetic field \vec{B} . In the above, μ_B is the Bohr magneton, \vec{S} is the spin angular momentum vector, and \mathbf{g} is the electronic g-tensor. Elements of \mathbf{g} are typically expressed as spatially dependent deviations from the free electron g value ($g_e \cong 2.002319$) as follows:

$$g^{ab} = g_e \delta^{ab} + \Delta g^{ab} \quad (2)$$

where $\mathbf{a}, \mathbf{b} \in \{x, y, z\}$ are Cartesian indices and Δg^{ab} reflects local environment perturbations on the spin magnetic moment of an unpaired electron. Δg^{ab} can be represented as a second-order perturbation expansion over a spin/field reduced Hamiltonian of Breit Pauli terms with linear \vec{S} and \vec{B} dependence.^{16,17}

$$\Delta g^{ab} = \Delta g_{\text{RMC}}^{ab} \delta^{ab} + \Delta g_{\text{GC-SZ}}^{ab}(\mathbf{1e}) + \Delta g_{\text{GC-SZ}}^{ab}(\mathbf{2e}) + \Delta g_{20}^{ab}(\mathbf{1e}) + \Delta g_{20}^{ab}(\mathbf{2e}) \quad (3)$$

In the above, Δg_{RMC} is the relativistic mass correction to the spin Zeeman, $\Delta g_{\text{GC-SZ}}(\mathbf{1e})$ and $\Delta g_{\text{GC-SZ}}(\mathbf{2e})$ are one- and two-electron gauge corrections to the spin Zeeman (also referred to as *diamagnetic* terms in analogy with magnetic susceptibility nomenclature), whereas $\Delta g_{20}(\mathbf{1e})$ and $\Delta g_{20}(\mathbf{2e})$ are magnetic response (*paramagnetic*) terms arising from one- and two-electron spin-orbit coupling within a field-perturbed wave

function. The latter may be computed in terms of SOS expansions,¹⁷ for example,

$$\Delta g_{20}^{ab}(\mathbf{1e}) = \frac{2}{M_S} \sum_i \frac{\langle \Phi_0 | H_{\text{SO}}^a(\mathbf{1e}) | \Phi_i \rangle \langle \Phi_i | H_{\text{OZ}}^b | \Phi_0 \rangle}{E_i - E_0} \quad (4)$$

where H_{SO}^a is the *a*th component of the one-electron spin-orbit operator, and H_{OZ}^b is the *b*th component of the orbital Zeeman operator. $\Delta g_{20}^{ab}(\mathbf{2e})$ is defined analogously by replacing $H_{\text{SO}}^a(\mathbf{1e})$ with the corresponding two-electron spin-orbit coupling operators. Expressions for the relevant terms and operators for all quantities in eqs 3 and 4 are given explicitly in numerous other references (e.g., ref 16) and need not be repeated here.

For MRCI-level g-tensor calculations^{3,4} the states $|\Phi_0\rangle$ and $|\Phi_i\rangle$ in eq 4 are all explicitly resolved MRCI wave functions.³ In the much simpler ROHF SOS methodology, however, they are approximated as single determinants, wherein $|\Phi_0\rangle$ corresponds to the HF ground state $|\Psi_0\rangle$, and excited configurations $|\Phi_i\rangle$ are obtained by promoting electrons from occupied to virtual orbitals in the ROHF ground-state basis. The corresponding denominator $E_i - E_0$ in eq 4 becomes simply the difference in energy between the two determinants.¹⁰

Although the ROHF technique gives only a rough approximation to the magnetic response, it does provide a convenient means for identifying the magnetically relevant configurations $|\Psi_n\rangle$ that produce significant contributions, that is, greater than some arbitrary threshold:

$$\Delta g^{ab}(\Psi_n) = \frac{2}{M_S} \left| \frac{\langle \Psi_0 | H_{\text{SO}}^a | \Psi_n \rangle \langle \Psi_n | H_{\text{OZ}}^b | \Psi_0 \rangle}{E_n - E_0} \right| \geq \text{Threshold} \quad (5)$$

to the ROHF SOS expansion for a particular g-shift Δg^{ab} . Because H_{OZ} is a one-electron operator, all double (or higher-order) excitations do not directly contribute and are thus excluded. As well, in higher-symmetry species, selection rules equivalent to those for interstate magnetic dipole coupling also apply and further restrict the configuration space. Because of these useful restrictions, the total number of configurations selected by such a screening process is typically rather small—at most $n_S(n_S - 1)$, where n_S is the number of molecular orbitals for the relevant symmetry.

Because of the relatively small number of these magnetically relevant configurations, it should often be possible to construct the complete manifold of corresponding CI wave functions as linear combinations of these $|\Psi_n\rangle$:

$$|\Phi_i\rangle = \sum_n c_{in} |\Psi_n\rangle \quad (6)$$

Substituting this expression into eq 4, and making the approximation $|\Phi_0\rangle \cong |\Psi_0\rangle$ gives:

$$\Delta g_{20}^{ab} = \frac{2}{M_S} \sum_i \frac{(\sum_a c_{ia} \langle \Psi_0 | H_{\text{SO}}^a | \Psi_a \rangle) (\sum_a c_{ia} \langle \Psi_a | H_{\text{OZ}}^b | \Psi_0 \rangle)}{E_i - E_0} \quad (7)$$

At this point we have a simple CI expression designed to model the correlated paramagnetic response of an uncorrelated ground state $|\Psi_0\rangle$. Because the complete CI manifold can generally be incorporated without great computational expense

TABLE 1: Theoretically Computed (MRCI) Excitation Energies for the First Excited State in Each Manifold Contributing to g-Shifts of NO₂, H₂O⁺, MgF, CO⁺, and H₂CO⁺

| | g-shift | first state | $\Delta E'_{0-1}$ (in eV) |
|---|---------|-------------------------------|---------------------------|
| NO ₂ (X ² A ₁) | xx | 1 ² B ₂ | 3.2056 ^a |
| | yy | 1 ² B ₁ | 3.3014 ^a |
| | zz | 1 ² A ₂ | 3.6224 ^a |
| H ₂ O ⁺ (X ² B ₁) | xx | 1 ² A ₂ | 15.4772 ^a |
| | yy | 1 ² A ₁ | 1.9951 ^a |
| | zz | 1 ² B ₂ | 6.4350 ^a |
| H ₂ CO ⁺ (X ² B ₂) | xx | 1 ² A ₁ | 5.278 ^b |
| | yy | 1 ² A ₂ | 9.885 ^b |
| | zz | 1 ² B ₁ | 3.860 ^b |
| CO ⁺ (X ² Σ ⁺) | ⊥ | 1 ² Π | 3.2450 ^a |
| MgF (X ² Σ ⁺) | ⊥ | 1 ² Π | 3.6282 ^c |

^a Ref 3. ^b Ref 18. ^c Ref 4.

(i.e., no truncations are necessary as per the MRCI method), this treatment is referred to herein as a *closed-form* expansion.

There is a technical problem with eq 7, however. Although the configuration space $|\Psi_n\rangle$ contains only single excitations relative to $|\Psi_0\rangle$, configurations within the space may either be single or double excitations with respect to each other. Because some states may be double excitations with respect to each other, the $|\Phi_i\rangle$ manifold possesses nonzero Coulomb correlation, which means that the E_i values may be unrealistically energetically depressed relative to the uncorrelated E_0 . The rigorous solution to this would be to use a multiconfigurational $|\Phi_0\rangle$ with the same level of correlation as the $|\Phi_i\rangle$ manifold. Unfortunately this would lead to a dramatic increase in computational expense, and satisfying the criterion of identical levels of correlation for $|\Phi_0\rangle$ and $|\Phi_i\rangle$ is nontrivial. Luckily, one may circumvent such problems empirically by simply shifting the entire set of E_i levels by a quantity ϵ such that the shifted value for the first excitation energy in the manifold reproduces some known value:

$$\Delta E'_{0-1} = E'_1 - E_0 = (E_1 + \epsilon) - E_0 \equiv \Delta E_{0-1} \text{ (known)} \quad (8)$$

Experimental vertical excitation energies should certainly suffice for the empirical $\Delta E'_{0-1}$ parameter; however, in this work we have chosen to use values determined theoretically via MRCI calculations^{3,4,18} as given in Table 1.

The number of different state manifolds for which $\Delta E'_{0-1}$ must be specified depends on the symmetry of the molecule. For systems with intermediate levels of symmetry (e.g., C_s , C_{2v} , D_{2h} , etc.), multiple $\Delta E'_{0-1}$ values must be specified, as different g-shifts entail coupling with state manifolds of different symmetry. For very high-symmetry systems (e.g., O_h , T_d , linear species, etc.), only one value is required, as the different relevant manifolds are energetically degenerate. Systems with no symmetry at all (i.e., C_1) also require specifying only one $\Delta E'_{0-1}$ because the excited manifold is always of the same symmetry (A) regardless of the g-shift to be computed.

Computational Details

In this work, g-tensors are reported for the following series of molecular radicals: NO₂, H₂O⁺, MgF, CO⁺, and H₂CO⁺. These particular systems have been chosen because of ample availability of both experimental and theoretical data for comparison. Calculations have been performed at the ROHF and closed-form CI (CFCI) levels using the GSTEPS suite of g-tensor computation codes.¹⁹ Compared with previous results,^{4,10} some differences occur in the ROHF-level g-tensor values reported herein. Although some of the deviation can be

attributed to the use of different basis sets, the main deviation arises from refinements to one of the GSTEPS algorithms that, for the sake of computational expediency, made (and attempted to exploit) the assumption:

$$\langle \chi_1 \chi_2 | \mathbf{H}_{\text{SO}}(\mathbf{2e}) | \chi_3 \chi_2 \rangle \cong -\langle \chi_3 \chi_2 | \mathbf{H}_{\text{SO}}(\mathbf{2e}) | \chi_1 \chi_2 \rangle \quad (9)$$

which (by straightforward algebra that need not be repeated here) can be shown to be of questionable reliability. For this reason, the current version of the GSTEPS code does not take this shortcut and thus computes both of the integrals in eq 9 explicitly.

The GSTEPS suite of programs is built atop the ROHF and CI programs available in the MRDCI package of Buenker, and co-workers.²⁰ It also incorporates some external integral evaluation codes, including the MAGOPS program of Augspurger and Dykstra²¹ and the Eagle program of Chandra, Buenker, Marian, and Hess.²²

The basis sets used in this study are all triple- ζ polarized constructs of Sadlej.²³ Geometries for NO₂, CO⁺, and MgF correspond to experimental values summarized elsewhere.^{3,4} In the absence of experimental structural data for H₂O⁺ and H₂CO⁺, theoretically optimized structures were used.^{3,18} In all cases, the molecular origin was specified to coincide with the electronic charge centroid (ECC) of the molecule (as determined from ROHF calculations). Choosing the ECC as gauge provides a consistent, nonarbitrary coordinate system for our gauge-dependent g-tensor methodology and, as shown by Luzanov et al.,²⁴ should lead to results that effectively approximate the ideal fully gauge-invariant values.

For the CFCI g-tensor calculations, initial tests were done with configuration spaces incorporating only those one-open-shell determinants for which magnetic coupling with the ground state was symmetry-allowed. This is to say that three-open-shell configurations were initially omitted under the rationale that g-shifts from the two projections of a given three-open-shell configuration tend to approximately cancel each other in the ROHF treatment.¹⁹ For refined calculations, however, studies were done on the effect in CFCI of including these additional configurations via a threshold selection formalism as per eq 5. For each system, initial calculations were performed using a threshold of 100 ppm. In the one poorly convergent case, H₂CO⁺, two further studies were done in which this threshold was lowered to 10 and 1 ppm, respectively.

Results and Discussion

Table 2 provides our ROHF level and CFCI g-tensor results for NO₂, H₂O⁺, H₂CO⁺, CO⁺, and MgF in detail. The first series of rows present the so-called *first-order* terms computed as expectation values over the ground-state ROHF wave functions. These include the relativistic mass correction and the one- and two-electron spin Zeeman gauge correction terms in eq 3. In general, such terms tend to have relatively small contributions to the total g-shifts, and previous work has demonstrated that their dependence on both basis sets¹⁰ and electron correlation³⁰ is relatively minor. For these reasons there is little motivation to treat them at levels higher than the current triple- ζ polarized ROHF scheme.

The ensuing set of rows in Table 2 report the ROHF-level SOS treatment of the one- and two-electron magnetic response contributions (see eqs 3 and 4). These terms are summed together along with the net first-order contributions to yield total ROHF-level g-shifts for each of the different species. As has been concluded elsewhere,^{4,10} the ROHF values typically tend

TABLE 2: ROHF and Closed-Form CI g-Tensor Calculations for NO₂, H₂O⁺, H₂CO⁺, CO⁺, and MgF^a

| | NO ₂ | | | H ₂ O ⁺ | | | H ₂ CO ⁺ | | | CO ⁺ | | MgF | |
|----------------------------|-----------------|----------|------|-------------------------------|----------|-------|--------------------------------|----------|-------|-----------------|------|----------|------|
| | xx | yy | zz | xx | yy | zz | xx | yy | zz | ⊥ | | ⊥ | |
| first-order | | | | | | | | | | | | | |
| Δg_{RMC} | -287 | -287 | -287 | -288 | -288 | -288 | -285 | -285 | -285 | -191 | -191 | -64 | -64 |
| $\Delta g_{\text{GC}}(1e)$ | 258 | 232 | 138 | 98 | 201 | 200 | 227 | 127 | 201 | 200 | 92 | 145 | 90 |
| $\Delta g_{\text{GC}}(2e)$ | -299 | -175 | -261 | -135 | -152 | -155 | -223 | -190 | -161 | -116 | -76 | -103 | -81 |
| total | -328 | -230 | -410 | -325 | -239 | -243 | -281 | -348 | -245 | -107 | -175 | -22 | -55 |
| ROHF response | | | | | | | | | | | | | |
| $\Delta g_{2o}(1e)$ | 4059 | -10059 | -266 | 0 | 22665 | 6486 | 5582 | -39 | 9634 | -1667 | 0 | -883 | 0 |
| $\Delta g_{2o}(2e)$ | -1140 | 3213 | 107 | 0 | -6809 | -2003 | -1639 | 34 | -2928 | 522 | 0 | 228 | 0 |
| total | 2591 | -7076 | -569 | -325 | 15617 | 3865 | 3663 | -353 | 6461 | -1252 | -175 | -677 | -55 |
| CI (1-open) response | | | | | | | | | | | | | |
| $\Delta g_{2o}(1e)$ | 5083 | -14345 | -296 | 0 | 25056 | 7451 | 9292 | -67 | 7235 | -2320 | 0 | -1503 | 0 |
| $\Delta g_{2o}(2e)$ | -1433 | 4552 | 117 | 0 | -7517 | -2299 | -2743 | 59 | -2206 | 758 | 0 | 372 | 0 |
| total | 3322 | -10023 | -589 | -325 | 17300 | 4984 | 6354 | -353 | 4784 | -1681 | -175 | -1153 | -55 |
| CI (1,3-open) response | | | | | | | | | | | | | |
| $\Delta g_{2o}(1e)$ | 4954 | -14415 | 53 | 23 | 25056 | 7755 | 9275 | -6 | 7235 | -3472 | 0 | -1499 | 0 |
| $\Delta g_{2o}(2e)$ | -1400 | 4574 | 24 | 0 | -7517 | -2379 | -2742 | 28 | -2206 | 1042 | 0 | 370 | 0 |
| total | 3785 | -10071 | -333 | -302 | 17300 | 5133 | 6252 | -326 | 4784 | -2537 | -175 | -1151 | -55 |
| expt. | | (ref 25) | | | (ref 26) | | | (ref 27) | | (ref 28) | | (ref 29) | |
| | 3800 | -11700 | 500 | 200 | 18800 | 4800 | 4600 | -800 | 200 | -2400 | | -1300 | -300 |
| | ±500 | ±500 | ±500 | ±500 | ±500 | ±500 | ±200 | ±200 | ±300 | ±400 | | ±500 | ±500 |

^a Threshold criterion of 100 ppm used for selecting three-open-shell configurations. All values in ppm.

to reproduce general trends in experimental g-shifts, but frequently exhibit significant quantitative discrepancies, often varying by upward of 50% from established experimental values for larger g-shifts. Furthermore, in the case of H₂CO⁺, we note a basic failure of the method to reproduce even qualitatively the small experimental Δg^{zz} . Such problems are not completely unexpected given the general difficulties in accurately reproducing excitation energies in eq 4 with an uncorrelated method.

Also reported in Table 2 are the magnetic response terms as computed via CFCI expansions. CFCI expansions including only one-open-shell configurations generally exhibit a major improvement relative to ROHF in terms of quantitative agreement with experiment. At this level, all g-shifts for H₂O⁺ and MgF are within (or just barely outside) the range of experimental uncertainty in the g-values. NO₂ and CO⁺, although not treated quite as accurately, are improved significantly over the ROHF-level values and bear reasonable quantitative accord with experiment. H₂CO⁺ results, however, are not appreciably better than those of ROHF and still exhibit the same major discrepancy for Δg^{zz} .

Addition of selected three-open-shell configurations, chosen according to eq 5 with contributions greater than 100 ppm, was generally found to improve the results. At this level, the Δg_{\perp} value for CO⁺ and the Δg^{xx} value for NO₂ are both brought effectively to within the experimental uncertainty ranges, whereas the quality of the results for H₂O⁺ and MgF was not significantly compromised. The Δg^{zz} value of H₂O⁺ was the only case where the additional three-open-shell configurations led to an appreciable decline in agreement with experiment; however, the small extent of this setback (149 ppm) raises little grounds for concern. Several cases, including the problematic Δg^{zz} value in H₂CO⁺, exhibit no change at all. In these cases the 100-ppm threshold for three-open-shell configurations is too high, permitting no further terms to be added to the configuration space.

To explore the limits of the CFCI methodology for resolving persistent trouble cases such as the Δg^{zz} shift in H₂CO⁺, further CFCI studies were done wherein the selection threshold was reduced to 10 and 1 ppm, respectively. These are reported in Figure 1, along with results from the one-open-shell and the 100-ppm threshold calculations. Because the small experimen-

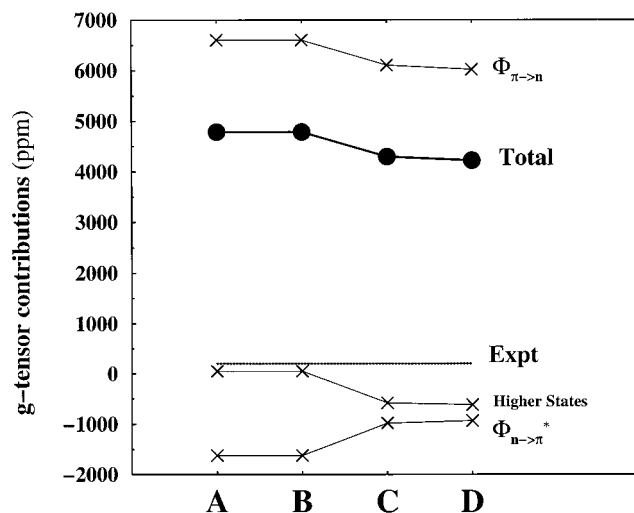


Figure 1. Δg^{zz} shifts for H₂CO⁺ as a function of CI expansion. Also reported are contributions due to ground-state magnetic coupling with $\Phi_{\pi \rightarrow n}$ and $\Phi_{n \rightarrow \pi^*}$, as well as the sum of contributions from higher states. All values in ppm. (A) One-open-shells only (12 configurations total). (B) Additional three-open-shells selected by threshold (thresh. = 100 ppm; 0 new configurations selected; 12 in total). (C) Additional three-open-shells selected by threshold (thresh. = 10 ppm; 18 new configurations selected; 30 in total). (D) Additional three-open-shells selected by threshold (thresh. = 1 ppm; 30 new configurations selected; 60 in total).

tally observed Δg^{zz} has been surmised to result from effective cancellation between the contributions of two states ($\Phi_{n \rightarrow \pi^*}$ and $\Phi_{\pi \rightarrow n}$) within the SOS expansion,¹⁸ the separate contributions of these two states have also been plotted. What one first sees in Figure 1 is the fact, already discussed, that no additional three-open-shell configurations are added to the space for the 100-ppm threshold and thus no improvement is achieved at this level. A 10-ppm threshold, however, permits the incorporation of 18 new configurations and ultimately leads to a drop in the Δg^{zz} value from 4784 to 4291 ppm—an improvement of 493 ppm. Although some of this effect does indeed arise from decreasing importance of $\Phi_{n \rightarrow \pi^*}$, whose contribution declines from +6602 to +6102 ppm, the degree of cancellation with $\Phi_{\pi \rightarrow n}$ actually changes very little in that the latter's contribution also declines

TABLE 3: Comparison of Different Theoretical g-Tensor Evaluation Techniques with Experimental Values for NO₂, H₂O⁺, H₂CO⁺, CO⁺, and MgF

| | | ROHF (this work) | CPHF (ref 11) | DFT (ref 12) | Small CI (this work) | MRCI (refs 3,4,18) | Expt (refs 25–29) |
|--------------------------------|------------------------|---------------------|------------------|-----------------|-------------------------|-----------------------|--------------------------|
| NO ₂ | Δg^{xx} | 2591 | 3368 | 4158 | 3785 | 3571 | 3800 ± 500 |
| | Δg^{yy} | -7076 | -11008 | -13717 | -10071 | -10296 | -11700 ± 500 |
| | Δg^{zz} | -569 | -623 | -760 | -333 | -537 | 500 ± 500 |
| H ₂ O ⁺ | Δg^{xx} | -325 | -229 | 103 | -302 | -249 | 200 ± 500 |
| | Δg^{yy} | 15617 | 12704 | 13824 | 17300 | 15733 | 18800 ± 500 |
| | Δg^{zz} | 3865 | 3306 | 5126 | 5133 | 4105 | 4800 ± 500 |
| H ₂ CO ⁺ | Δg^{xx} | 3663 | 5472 | 6231 | 6252 | 5510 | 4600 ^b ± 200 |
| | Δg^{yy} | -353 | 927 | -1220 | -326 | -50 | -800 ^b ± 200 |
| | Δg^{zz} | 6461 | 2976 | 76 | 4219 ^a | 1296 | 200 ^b ± 300 |
| CO ⁺ | Δg_{\perp} | -1252 | -2798 | -3129 | -2537 | -2383 | -2400 ± 400 |
| | Δg_{\parallel} | -175 | -42 | -138 | -175 | -178 | |
| | Δg_{\perp} | -677 | -1314 | -2178 | -1151 | -1092 | -1300 ^b ± 500 |
| MgF | Δg_{\perp} | -55 | 20 | -60 | -55 | -59 | -300 ^b ± 500 |
| | Δg_{\parallel} | 1641 | 1364 | 1090 | 949 | 844 | |
| Error ^c | | | | | | | |

^a Three-open-shell configurations selected according to a 1-ppm threshold. All values in ppm. ^b Matrix isolation (not gas phase) data; precise quantification of matrix effects unavailable. ^c Mean absolute deviation (in ppm) from experimental median value.

in (negative) magnitude from -1621 to -985 ppm. Rather, the net improvement in the results at the 10-ppm threshold depends more on the description of higher excited states (primarily the 3²B₁, 4²B₁ and 5²B₁ states of mixed character), whose net contribution shifts from +48 ppm to -581 ppm. The trend continues when going to a larger expansion as derived from a 1-ppm threshold criterion; however, the result ($\Delta g^{zz} = 4219$ ppm) is only slightly better, despite requiring the treatment of another 30 configurations beyond those selected for the 10-ppm threshold. It thus appears that the CFCI methodology does not converge to the correct answer in this case.

Table 3 provides an overview of the results for g-tensor calculations by assorted high-level methodologies including the ROHF and CFCI results produced in this work, MRCI values,^{3,4,18} CPHF computations of Jayatilaka,¹¹ and DFT values from the work of Schreckenbach and Ziegler.¹² These are all compared with an assortment of experimentally determined g-shifts. Because all of the theoretical numbers correspond to isolated molecules, we compare wherever possible with gas-phase experimental data.^{25,26,28} In the absence of gas-phase data (e.g., H₂CO⁺ and MgF), we compare with noble gas matrix isolation results,^{27,29} which should probably not vary by much more than 500–800 ppm from the gas-phase values.^{27,28}

To provide some rough quantification of the quality of the different theoretical methods, mean absolute deviations from experiment are reported. The statistical sample herein is too small (five molecules) to provide a firm foundation for pronouncements on the relative accuracy of the different methods; however, the general trends are still worthy of note. As should be expected, ROHF generally yields the poorest agreement with experiment, whereas MRCI gives the best. Despite the aforementioned problems with the Δg^{zz} value of H₂CO⁺, the CFCI methodology reported in this work appears to perform very respectably in comparison with the other methods. For this sample of systems, the CFCI results are somewhat better than those of either CPHF or DFT, and are actually only slightly worse on average than the MRCI.

Like many theoretical methodologies for g-tensor prediction, our model is inherently gauge dependent. Choice of the ECC as center of the computational coordinate system provides a partial remedy for the gauge problem,²⁴ but is only an approximate solution. To ensure reliable unambiguous results, therefore, the variation of g-tensor values with shifts in gauge must be demonstrably low. From Table 4, it would appear that this holds most of the time: gauge shifts from the ECC to a

TABLE 4: Gauge Dependences Expressed as Deviation (in ppm) of Δg -Values Arising from a Gauge Transformation of (1,1,1) Bohr from Electronic Charge Centroid of a Molecule

| | | gauge shift | relative to Δg (%) |
|--------------------------------|------------------------|-------------|----------------------------|
| NO ₂ | Δg^{xx} | -817 | 21.6 |
| | Δg^{yy} | 446 | 4.4 |
| | Δg^{zz} | 0 | 0 |
| H ₂ O ⁺ | Δg^{xx} | -20 | 6.6 |
| | Δg^{yy} | -248 | 1.4 |
| | Δg^{zz} | 0 | 0 |
| H ₂ CO ⁺ | Δg^{xx} | 188 | 3.0 |
| | Δg^{yy} | 14 | 4.3 |
| | Δg^{zz} | 0 | 0 |
| CO ⁺ | Δg_{\perp} | 122 | 4.8 |
| | Δg_{\parallel} | 0 | 0 |
| | Δg_{\perp} | -123 | 10.7 |
| MgF | Δg_{\perp} | -123 | 10.7 |
| | Δg_{\parallel} | 0 | 0 |

point (1,1,1) Bohr away lead to g-tensor fluctuations less than the experimental uncertainty in all cases except the Δg^{xx} value of NO₂. Gauge dependence in the latter (-817 ppm) is still only a modest fraction of the total Δg^{xx} value (3785 ppm), and thus should not pose any great concern regarding the CFCI method's ability to predict the basic experimental trend. However, any future application of the method to extended systems, especially those for which precise determination of an ECC is nontrivial, would be advised to monitor the magnitude of the gauge dependence relative to desired accuracy level.

Summary and Conclusions

In this work, a new configuration interaction methodology has been developed for the computation of electronic g-tensors. The methodology builds upon an ROHF-level SOS expansion of molecular magnetic response from which one can pinpoint configurations that magnetically couple with the ground state. Assembling these configurations together yields a magnetically relevant configuration space, generally much smaller than those used for more general CI calculations (e.g., CI Singles and Doubles, MRCI). Given the modest size of the space, it is often feasible to generate the entire set of excited states arising as linear combinations of these determinants, and to perform a closed-form SOS g-tensor expansion over this manifold. This methodology provides a means for a partially correlated treatment of the (often dominant) magnetic response component of the g-tensor expansion at a computational expense that, for many systems of interest, differs little from that of the original ROHF-level calculations. This new technique has been referred to in this work as the CFCI method for g-tensor calculation.

On the basis of the availability of ample prior experimental and theoretical data, a series of test molecules, namely NO_2 , H_2O^+ , H_2CO^+ , CO^+ , and MgF , was chosen for benchmarking the CFCI methodology. New ROHF-level results, obtained in this work as a necessary computational precursor to the CFCI calculations, have also been reported.

One useful feature of the CFCI method is an inherent flexibility in computational complexity that is manifested in the way one selects the configuration space. Restricting the space to one-open-shell configurations leads to a small, computationally trivial CI expansion that yields results markedly better than those of ROHF and generally quite comparable with experiment. Addition of threshold-selected three-open-shell configurations, however, yields appreciable further improvement, often ameliorating the agreement by several hundred ppm. A 100-ppm threshold for three-open-shell configuration selection leads to fair quantitative agreement with experiment in the majority of cases. The only major exception that we have encountered thus far is the Δg^{zz} value of H_2CO^+ , in which theory (4784 ppm) and experiment (200 ppm) display a drastic discrepancy. Lowering the threshold to 10 ppm, thereby adding 18 configurations to the expansion, reduces the discrepancy by 493 ppm but still leaves a fundamental qualitative disagreement between experiment and theory. Little additional improvement is achieved with smaller selection thresholds. This particular case has already attained a certain degree of notoriety in the literature,^{9,11,18} and the only techniques to provide plausible agreement with experiment are MRCI¹⁸ and DFT.¹² From this, one can surmise the H_2CO^+ problem to be resolved only through use of highly correlated techniques.

Despite the Δg^{zz} discrepancy with H_2CO^+ , the CFCI method compares very favorably with the other theoretical techniques currently available for g-tensor computation. Although the suite of test cases may not be not large enough to support firm assessments of the relative accuracy of the different methods, one can make general assertions such as the CPHF, DFT, and CFCI techniques all appearing to be significantly better than the ROHF SOS formalism. Given as evidence the mean absolute discrepancies between theoretical and experimental values for the g-shifts in this test suite, the CFCI technique (mean error of 949 ppm) may prove somewhat more reliable than either the DFT (1090 ppm) or CPHF (1364 ppm) methods. Although MRCI (mean error of 844 ppm) is marginally superior for the small radicals studied herein, the technique can be cumbersome for large systems because of computational expense and inherent difficulties in unambiguous selection of relevant excited states in larger manifolds. For reasons such as this, the future of g-tensor analysis, which may focus increasingly on complex systems such as biradicals and solid-state defects, is more likely to require computationally expedient and straightforward techniques such as the CPHF, DFT, and CFCI methodologies.

Acknowledgment. This work was conducted as part of the Programming Environment and Training initiative within the U.S. Department of Defense High Performance Computing Modernization Program. Pablo Bruna, Friedrich Grein, and Shashi Karna are all gratefully acknowledged for their helpful suggestions, and for providing impetus for this work.

References and Notes

- (1) Atkins, P. W. *Molecular Quantum Mechanics*; Oxford University Press: New York, 1983, and references therein.
- (2) Lushington, G. H.; Bruna, P. J.; Grein, F. Z. *Phys. D: At., Mol. Clusters* **1996**, *36*, 301.
- (3) Lushington, G. H.; Grein, F. *J. Chem. Phys.* **1997**, *106*, 3292.
- (4) Lushington G. H.; Grein, F. *Int. J. Quantum Chem.* **1996**, *60*, 467.
- (5) Bruna, P. J.; Lushington, G. H.; Grein, F. *Chem. Phys.* **1997**, *225*, 1.
- (6) Bruna, P. J.; Grein, F. *J. Phys. Chem.* **1999**, *103*, 3294.
- (7) Sherrill, C. D.; Schaefer, H. F. *Adv. Quantum Chem.* **1999**, *34*, 143.
- (8) Moores, W. H.; McWeeny, R. *Proc. R. Soc. London, Ser. A* **1973**, *332*, 365.
- (9) Ishii, M.; Morihashi, K.; Kikuchi, O. *J. Mol. Struct.: THEOCHEM* **1991**, *325*, 39.
- (10) Lushington, G. H.; Grein, F. *Theor. Chim. Acta* **1996**, *93*, 259.
- (11) Jayatilaka, D. *J. Chem. Phys.* **1998**, *108*, 7587.
- (12) Schreckenbach, G.; Ziegler, T. *J. Phys. Chem.* **1997**, *101*, 3388.
- (13) van Lenthe, E.; Wormer, P. E. S.; van der Avoird, A. *J. Chem. Phys.* **1997**, *107*, 2488.
- (14) Vahtras, O.; Minaev, B.; Ågren, H. *Chem. Phys. Lett.* **1997**, *281*, 186.
- (15) Krylov, A. I.; Sherrill, C. D.; Head-Gordon, M. *J. Chem. Phys.* **1998**, *109*, 10669.
- (16) Harriman, J. E. *Theoretical Foundations of Electron Spin Resonance*; Academic Press: New York, 1978.
- (17) McWeeny, R. *Methods of Molecular Quantum Mechanics*, 2nd ed.; Academic Press: London, 1989.
- (18) Bruna, P. J.; Lushington, G. H.; Grein, F. *J. Mol. Struct.: THEOCHEM*, in press.
- (19) Lushington, G. H. PhD Thesis, University of New Brunswick, Canada, 1996.
- (20) Buenker, R. J.; Peyerimhoff, S. D.; Butscher, W. *Mol. Phys.* **1978**, *35*, 771; Knowles, D. B.; Alvarez-Collado, J. R.; Hirsch, G.; Buenker, R. *J. J. Chem. Phys.* **1990**, *92*, 585.
- (21) Augspurger, J. D.; Dykstra, C. E. *J. Comput. Chem.* **1990**, *11*, 105.
- (22) Chandra, P.; Buenker, R. J. *J. Chem. Phys.* **1983**, *79*, 358, 366; Marian, C. M. Diplomarbeit, University of Bonn, Germany, 1977 and Doktorarbeit, University of Bonn, Germany, 1981; Hess, B. A. Diplomarbeit, University of Bonn, Germany, 1977 and Doktorarbeit, University of Bonn, Germany, 1981.
- (23) Sadlej, A. J. *Collect. Czech. Chem. Commun.*, **1988**, *53*, 1995; *J. Mol. Struct.: THEOCHEM* **1991**, *234*, 147.
- (24) Luzanov, A. V.; Babich, E. N.; Ivanov, V. V. *J. Mol. Struct.: THEOCHEM* **1994**, *311*, 211.
- (25) Brown, J. M.; Steimle, T. C.; Coles, M. E.; Curl, R. F. *J. Chem. Phys.* **1981**, *74*, 3668.
- (26) Knight, L. B.; Steadman, J. *J. Chem. Phys.* **1983**, *78*, 5940.
- (27) Knight, L. B.; Steadman, J. *J. Chem. Phys.* **1984**, *80*, 1018.
- (28) Knight, L. B.; Steadman, J. *J. Chem. Phys.* **1982**, *77*, 1750. *J. Am. Chem. Soc.* **1984**, *106*, 900.
- (29) Knight, L. B.; Easley, W. C.; Weltner, W. *J. Chem. Phys.* **1971**, *54*, 322.
- (30) Bündgen, P.; Lushington, G. H.; Grein, F. *Int. J. Quantum Chem. Symp.* **1995**, *29*, 283.